# Targeted delivery of a cisplatin prodrug for safer and more effective prostate cancer therapy in vivo

Shanta Dhar[a,1], Nagesh Kolishetti[b,c,1], Stephen J. Lippard[a,d,2], and Omid C. Farokhzad[b,c,2]

[a]Department of Chemistry, Massachusetts Institute of Technology, Cambridge, MA 02139; [b]Laboratory of Nanomedicine and Biomaterials, Department of Anesthesiology, Brigham and Women's Hospital (BWH), Harvard Medical School, 75 Francis Street, Boston, MA 02115; [c]Massachusetts Institute of Technology (MIT)–Harvard Center for Cancer Nanotechnology Excellence, Massachusetts Institute of Technology, 77 Massachusetts Avenue, Cambridge, MA 02139; and [d]Koch Institute for Integrative Cancer Research, Massachusetts Institute of Technology, 77 Massachusetts Avenue, Cambridge, MA 02139

Edited by Chad A. Mirkin, Northwestern University, Evanston, IL, and approved December 6, 2010 (received for review August 1, 2010)

**Targeted delivery and controlled release of inactive platinum (Pt) prodrugs may offer a new approach to improve the efficacy and tolerability of the Pt family of drugs, which are used to treat 50% of all cancers today. Using prostate cancer (PCa) as a model disease, we previously described the engineering of aptamer (Apt)-targeted poly(D,L-lactic-*co*-glycolic acid)-*b*-poly(ethylene glycol) (PLGA-*b*-PEG) nanoparticles (NPs) encapsulating a Pt(IV) prodrug *c,t,c*-[Pt(NH$_3$)$_2$-(O$_2$CCH$_2$CH$_2$CH$_2$CH$_2$CH$_3$)$_2$Cl$_2$] (1) (Pt-PLGA-*b*-PEG-Apt-NP), which target the extracellular domain of the prostate specific membrane antigen (PSMA), for enhanced in vitro cytotoxicity. Here we demonstrate enhanced in vivo pharmacokinetics (PK), biodistribution, tolerability, and efficacy of Pt-PLGA-*b*-PEG-Apt-NP (150±15 nm encapsulating ∼5% wt/wt Pt(IV) prodrug) when compared to cisplatin administered in its conventional form in normal Sprague Dawley rats, Swiss Albino mice, and the PSMA-expressing LNCaP subcutaneous xenograft mouse model of PCa, respectively. The 10-d maximum tolerated dose following a single i.v. injection of Pt-PLGA-*b*-PEG-NP in rats and mice was determined at 40 mg/kg and 5 mg/kg, respectively. PK studies with Pt-PLGA-*b*-PEG-NP revealed prolonged Pt persistence in systemic blood circulation and decreased accumulation of Pt in the kidneys, a major target site of cisplatin toxicity. Pt-PLGA-*b*-PEG-Apt-NPs further displayed the significant dose-sparing characteristics of the drug, with equivalent antitumor efficacy in LNCaP xenografts at 1/3 the dose of cisplatin administered in its conventional form (0.3 mg/kg vs. 1 mg/kg). When considering the simultaneous improvement in tolerability and efficacy, the Pt-PLGA-*b*-PEG-Apt NP provides a remarkable improvement in the drug therapeutic index.**

chemotherapy | metals in medicine | biodegradable polymer | nanomedicine

Chemotherapy is standard treatment of most disseminated cancers, but dose-limiting toxicities and the emergence of cancer cells resistant to chemotherapeutic drugs often reduce the clinical benefit (1). Cisplatin is one of the most effective chemotherapeutic agents against many forms of cancer including testicular, bladder, head and neck, ovarian, breast, lung, prostate, and refractory non-Hodgkin's lymphomas (2, 3). Indeed, cisplatin is used to treat 50% of all cancers (4), and it exerts its antitumor effects by disrupting DNA structure in cell nuclei through the formation of intrastrand and interstrand cross-links (5). Despite the ubiquitous use of cisplatin in oncology, this drug is associated with significant dose-limiting toxicities including nephrotoxicity and neurotoxicity. There is correspondingly a clear incentive to develop new strategies for safer and more effective cisplatin herapy. Our previous work demonstrated the benefits of aptamer-targeted polymeric nanoparticles (NPs) to deliver drugs when compared to equivalent nontargeted nanoparticles, or to drugs given in their conventional dosage form, by (*i*) delivering a higher total fraction of drugs to tumors; (*ii*) enhancing intracellular drug delivery through receptor mediated endocytosis; (*iii*) enhancing anticancer efficacy in vitro and in vivo (6–8). More recently we described a platinum (Pt) (IV) prodrug, which, when delivered via targeted polymeric NPs, resulted in enhanced cytotoxicity in cell culture (9). This construct was successfully directed to prostate cancer (PCa) cells in vitro by targeting the prostate specific membrane antigen (PSMA) on androgen-sensitive LNCaP human prostate adenocarcinoma cells (9–14). Controlled release NPs derived from poly(D,L-lactic-*co*-glycolic acid)-*b*-poly (ethylene glycol) (PLGA-*b*-PEG) have a significantly prolonged circulation half-life when compared to similar particles lacking PEG (15, 16). The hydrophobic Pt(IV) prodrug *c,t,c* – [Pt(NH$_3$)$_2$ (O$_2$CCH$_2$CH$_2$CH$_2$CH$_2$CH$_3$)$_2$Cl$_2$] (**1**, Scheme 1), which releases the more hydrophilic cisplatin after reduction of the Pt(IV) in the cells (17–20), also facilitated encapsulation of the compound in the hydrophobic core of PLGA-*b*-PEG NPs. Surface functionalization of the PLGA-*b*-PEG NPs with the A10 PSMA aptamer (Apt) (7) allowed us to successfully target prostate cancer using Pt-PLGA-*b*-PEG-Apt-NPs with superior efficacy compared to cisplatin administered in its conventional form (9, 20).

Here we report that targeted delivery of cisplatin in the form of a prodrug **1** using a NP delivery system can markedly improve its tolerability and efficacy in vivo. Our studies have broad implications for cancer therapy given the relatively ubiquitous use of cisplatin in oncology, and they suggest that similar strategies be undertaken to combine prodrugs with targeted delivery to synergistically improve safety and efficacy.

## Results and Discussion

**Development of Pt-PLGA-*b*-PEG-Apt-NPs.** Pt-encapsulated NPs Pt-PLGA-*b*-PEG-NPs were prepared by nanoprecipitation as previously reported (9). The NP size distribution was determined by dynamic light scattering. Platinum loading was determined by flameless atomic absorption spectroscopy (AAS). The average size of the NPs was $150 \pm 15$ nm and the average loading efficiency was ∼5%. Surface functionalization of the Pt-PLGA-*b*-PEG NPs with the A10 PSMA Apt was achieved under standard amide coupling conditions in the presence of 1-ethyl-3-[3-dimethylaminopropyl]carbodiimide hydrochloride (EDC) and NHS (6, 7, 17).

Author contributions: S.D., N.K., S.J.L., and O.C.F. designed research; S.D. and N.K. performed research; S.D. and N.K. contributed new reagents/analytic tools; S.D., N.K., S.J.L., and O.C.F. analyzed data; and S.D., N.K., S.J.L., and O.C.F. wrote the paper.

Conflict of interest statement: In compliance with the Brigham and Women's Hospital and Harvard Medical School institutional guidelines, O.C.F. discloses his financial interest in BIND Biosciences and Selecta Biosciences, two biotechnology companies developing nanoparticle technologies for medical applications. BIND and Selecta did not support the aforementioned research, and currently these companies have no rights to any technology or intellectual property developed as part of this research.

This article is a PNAS Direct Submission.

[1]S.D. and N.K. contributed equally to this work.

[2]To whom correspondence may be addressed. E-mail: lippard@mit.edu or ofarokhzad@zeus.bwh.harvard.edu.

This article contains supporting information online at www.pnas.org/lookup/suppl/doi:10.1073/pnas.1011379108/-/DCSupplemental.

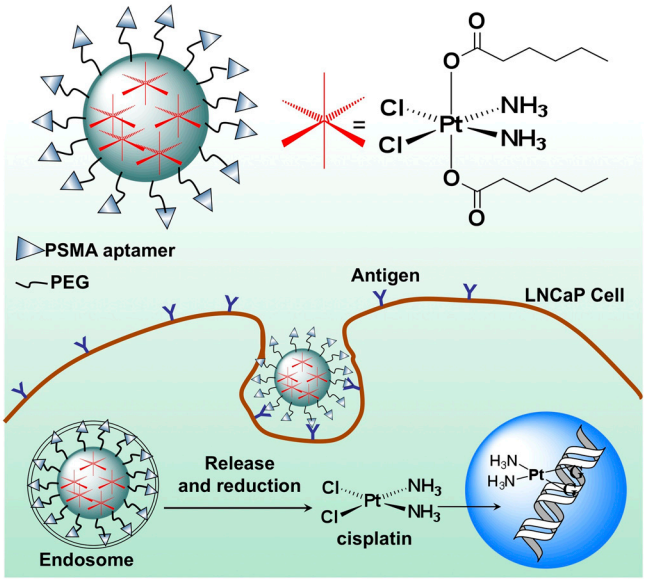


**Scheme 1.** Schematic representation of the Pt-PLGA-*b*-PEG-Apt-NP construct. Chemical structure of the Pt(IV) prodrug **1** and intracellular reduction for the release of active cisplatin in PSMA expressing human prostate cancer LNCaP cells after receptor mediated endocytosis of Pt-PLGA-*b*-PEG-Apt-NP.

**Table 1. Dosing information for MTD studies in rats**

| Dose, mg/kg | No. of rats | Death |
|---|---|---|
| Pt-PLGA-*b*-PEG-NP | | |
| 5 | 3 | 0 |
| 10 | 3 | 0 |
| 20 | 3 | 0 |
| 40 | 3 | 0 |
| 50 | 3 | 2 |
| 60 | 3 | 2 |
| Pt(IV) prodrug, **1** | | |
| 5 | 3 | 0 |
| 10 | 3 | 0 |
| 20 | 3 | 0 |
| 40 | 3 | 2 |
| PLGA-*b*-PEG-NP | | |
| 100 | 3 | 0 |
| 200 | 3 | 0 |
| 400 | 3 | 0 |
| 800 | 3 | 0 |
| 1,000 | 3 | 0 |

**In Vivo Toxicity.** We examined the maximum tolerated dose (MTD) of various doses of cisplatin, the Pt(IV) prodrug, Pt-PLGA-*b*-PEG-NPs, or PLGA-*b*-PEG-NPs after a single i.v. injection into male Sprague Dawley Rats. The MTD was estimated based on the threshold at which all animals survived (Fig. 1*A*). Dosing and survival details are summarized in Table 1. All rats treated with control NPs tolerated these doses. In the Pt-PLGA-*b*-PEG-NP group, rats receiving doses up to 40 mg/kg tolerated the dose, but two of three, respectively, in the 50- and 60-mg/kg groups died. Only a dose of 20 mg/kg of cisplatin or the Pt(IV)-prodrug was tolerated by the rats. To further define the MTD, the overall toxicity as revealed by body weights was monitored over 10 d (Fig. 2). For cisplatin, only rats receiving a dose of 20 mg/kg had significant weight loss, whereas those receiving lower doses did not. For Pt-PLGA-*b*-PEG-NP and PLGA-*b*-PEG-NP, rats receiving all the different doses showed normal weight gain. For all rats receiving the Pt(IV)-prodrug up to 20 mg/kg, there was no weight loss. We therefore conclude that the MTD for Pt-PLGA-*b*-PEG-NP is 40 mg/kg and that of cisplatin and Pt(IV)-prodrug is 20 mg/kg.

The tolerance of Swiss Albino mice to different doses of Pt(IV)-prodrug-loaded PLGA-*b*-PEG-NPs was also investigated (Fig. 1*B*). Five groups ($n = 3$) of mice were given a single intravenous injection of Pt-PLGA-*b*-PEG-NP with Pt contents of 1 mg/kg, 3 mg/kg, 5 mg/kg, and 10 mg/kg. For three dose levels tested (1, 3, and 5 mg/kg based on Pt), all mice showed normal weight gain during a period of 11 d. A small reduction in weight was observed only in the group of mice treated with a 10 mg/kg dose of Pt-loaded NPs. Control mice treated with 200 mg/kg of control PLGA-*b*-PEG-NP did not show any significant weight change. During the observation period, no deterioration in health was observed in mice treated with 5 mg/kg Pt-loaded or control NPs, and the overall behavior was no different compared to that observed for untreated animals. The MTD of Pt-PLGA-*b*-PEG-NP in mice is >5 mg/kg vs. the previously reported MTD of cisplatin in mice, 4 mg/kg (21). Although cisplatin is one of the most effective anticancer drugs in use today, it conveys considerable toxicity to patients (4). Our data suggest that targeted PLGA-*b*-PEG-NPs may have fewer side effects as compared to cisplatin in its conventional dosage form. Based on survival (Fig. 1) and the body weight measurements in mice and rats during treatment (Fig. 2), the Pt(IV)-prodrug-loaded NPs appeared to be better tolerated than cisplatin in its conventional dosage form.

Alterations of clinical chemistry parameters in rats after treatment with Pt-PLGA-*b*-PEG-NPs, **1**, and cisplatin are shown in Fig. 3 and Table S1. Administration of Pt-loaded NPs did not affect the blood urea nitrogen (BUN) and creatinine levels by comparison to the groups treated with saline (0 mg/kg) (Fig. 3). For cisplatin-treated groups, changes in the clinical chemistry parameters indicated renal toxicity. The level of BUN and creatinine was increased for groups treated with cisplatin at a dose of 20 mg/kg. It is very interesting to note that the renal toxicity after treatment with high doses of Pt-PLGA-*b*-PEG-NPs is less than that of cisplatin in its conventional dosage form. No significant differences were observed between the groups treated with the prodrug **1** and Pt-loaded NPs. These observations indicate that

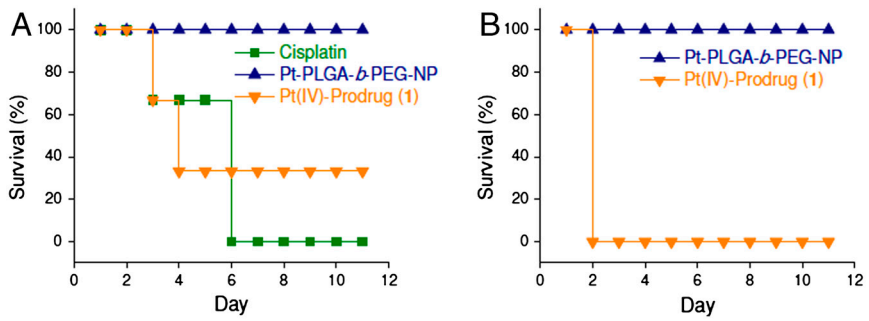


**Fig. 1.** Survival rate of (*A*) Sprague Dawley rats treated with cisplatin, Pt-PLGA-*b*-PEG-NPs, and **1** and (*B*) Swiss Albino mice treated with Pt-PLGA-*b*-PEG-NPs, and **1**.

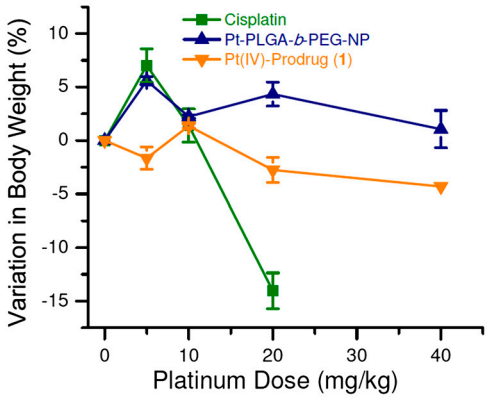


**Fig. 2.** Body weight variations observed for 10 d after intravenous administration of cisplatin, Pt-PLGA-*b*-PEG-NPs, and Pt(IV) prodrug **1** in male Sprague Dawley rats.

the Pt-PLGA-*b*-PEG-NP treatment is able to mitigate the nephrotoxicity that is attributed to cisplatin. The treatment of rats with cisplatin at a dose of 40 mg/kg shows an increased level of aspartate aminotransferase (AST) indicating the appearances of hepatotoxicity (Fig. 3). There was no effect on the total protein, albumin, and globulin after treatment with cisplatin in its conventional dosage form, **1**, or Pt-loaded NPs. These results reveal significant differential toxicity profiles for Pt-PLGA-*b*-PEG-NPs and cisplatin as well as the beneficial effects of polymeric NPs in reducing its commonly encountered toxicities.

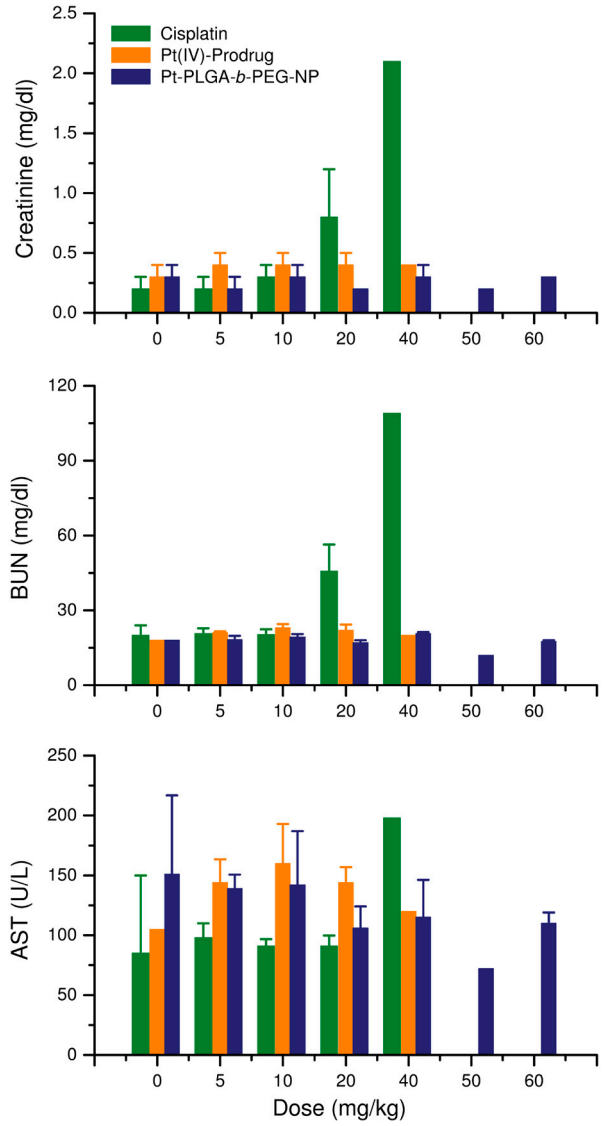


**Fig. 3.** Alterations of creatinine, BUN, and AST in rats after treatment with Pt-PLGA-*b*-PEG-NPs, **1**, or cisplatin.

**Biodistribution and Excretion In Vivo.** The comparative distribution and excretion of Pt-PLGA-*b*-PEG-NPs and the Pt(IV) prodrug **1** were investigated in male Sprague Dawley rats following intravenous administration of the maximally tolerated doses of the compounds. The variation of Pt levels in blood with time after intravenous administration of PLGA-*b*-PEG-NPs loaded with **1** and free **1** is shown in Fig. 4. Most small molecule anticancer drugs currently in clinical use, including cisplatin, doxorubicin, and paclitaxel, are inherently associated with lack of tumor selectivity and short blood circulation time, which causes various toxic side effects (22). In particular, cisplatin has an unfavorable pharmacokinetic (PK) profile, and all Pt-based anticancer drugs with a low molecular weight have a short half-life in the blood circulatory system (22, 23). The encapsulation of cisplatin in the form of a prodrug resulted in a significant prolongation of Pt presence in blood. Thus, Pt remaining in systemic circulation 1 h postadministration was 77% in the case of the Pt-PLGA-*b*-PEG-NPs and 15.6% in the case of free **1**, whereas the literature value for cisplatin is only 1.5% (23). The rate of Pt removal from blood was lower in the case of our system compared to a previously reported cisplatin-loaded PLGA-mPEG nanoparticle (23). Our studies also showed that most of the Pt in the blood is plasma bound (Fig. 4), a favorable indication for Pt being available to reach the target tumor sites. Prolonged drug residence in blood following intravenous administration of Pt prodrug-loaded NPs is a

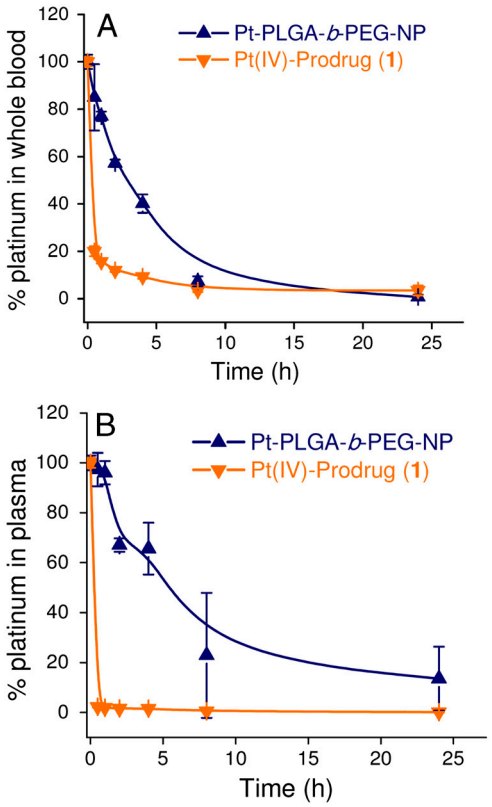


**Fig. 4.** Variation of percentage Pt dose in blood (*A*) and plasma (*B*) with time following the administration of Pt-PLGA-*b*-PEG-NPs and Pt prodrug **1** intravenously to rat.

**Table 2. Pharmacokinetic parameters for Pt-PLGA-*b*-PEG-NPs and 1**

| Test article | $AUC_{0-24\,h}$, h·ng/mL | $C_{max}$, ng/mL | $T_{max}$, h | CL, mL/h | $V_d$, mL/kg |
|---|---|---|---|---|---|
| Pharmacokinetic parameters in plasma | | | | | |
| Pt-PLGA-*b*-PEG-NPs | 48,915.08 | 6,477.0 | 0.5 | 3.6 | 43.2 |
| **1** | 14,742.37 | 1,181.4 | 0.5 | 6.6 | 210.9 |
| Pharmacokinetic parameters in blood | | | | | |
| Pt-PLGA-*b*-PEG-NPs | 12,735.77 | 3,128.3 | 0.5 | 16.74 | 81.87 |
| **1** | 3,851.55 | 646.7 | 0.5 | 37.9 | 678.7 |

AUC, area under curve; $C_{max}$, maximum concentration observed; $T_{max}$, time at maximum concentration; CL, clearance; $V_d$, volume of distribution.

prerequisite for the application of the PLGA-*b*-PEG-NPs in controlled intravenous delivery of cisplatin in the form of a prodrug for prostate cancer treatment. Individual PK parameters for Pt-PLGA-*b*-PEG-NPs and **1** are presented in Table 2. The mean area under curve (AUC) for total Pt in the blood is about 26% of that seen in plasma (Table 2), suggesting that Pt does not distribute extensively in red blood cells. The mean time to maximum serum concentration ($T_{max}$) was 0.5 h for both Pt-PLGA-*b*-PEG-NPs and **1**.

The comparative tissue distributions of Pt-PLGA-*b*-PEG NPs and **1** are shown in Fig. 5. After a single intravenous dose of Pt-PLGA-*b*-PEG-NPs, both the liver and spleen showed the highest Pt concentration at 24 h (Fig. 5). Statistical analyses of these data were performed using one-way ANOVA with Tukey post hoc test, $P < 0.05$ (compared with control). In the kidney, the primary target organ of cisplatin toxicity, Pt-PLGA-*b*-PEG-NPs showed lower Pt levels than the free prodrug **1**. The lower Pt level in the kidney indicated that our system will have reduced nephrotoxicity compared to that of cisplatin. The Pt(IV)-prodrug, **1**, showed a very similar distribution pattern to that typically exhibited by Pt compounds including cisplatin, the maximum concentration of Pt occurring in the kidney and liver. Because most of the Pt compound is retained in the nanoparticle core, the total amount of Pt measured in the Pt-PLGA-*b*-PEG-NP treated group is not equivalent to that of **1** that can react with biological substances with a pharmacological or toxicological efficacy. Prodrug encapsulated in NPs was released gradually with time, and tissues were continuously exposed to a low-dose drug environment. This effect could avoid high peak levels of cisplatin that might produce a severe toxicological effect.

We also determined the Pt content in the urine and feces after 24 h of cumulative excretion by atomic absorption spectroscopy. Excretion of Pt-PLGA-*b*-PEG-NPs was much lower than that of the prodrug **1**. The 24-h cumulative Pt excretion after Pt-PLGA-*b*-PEG-NPs is about 17 times less than after cisplatin treatment ($2.9 \pm 1.6$ vs. $50.3 \pm 3.7\%$) (21). This difference is due to the characteristics of Pt compounds, which can bind to protein or other tissue compositions firmly through covalent bonds. These results indicate that polymeric NPs are desirable delivery vehicles for Pt drugs.

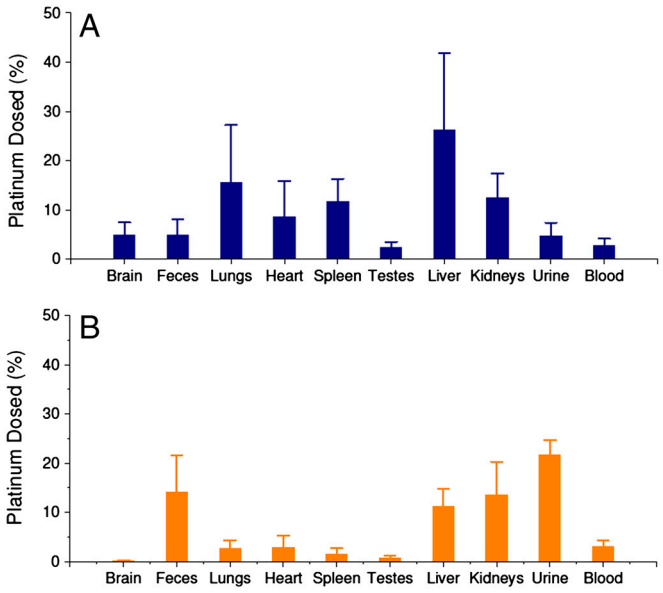


**Fig. 5.** Tissue distribution of (*A*) Pt-PLGA-*b*-PEG-NPs, and (*B*) free Pt(IV) prodrug **1** in male rats. Statistical analyses were performed using one-way ANOVA with Tukey post hoc test, $p < 0.05$ (compared with control).

**In Vivo Efficacy and Tolerability Using a LNCaP Subcutaneous Xenograft Mouse Model of PCa.** We next studied the efficacy of our Apt-targeted Pt-encapsulated NPs (Pt-PLGA-*b*-PEG-Apt-NP) using a xenograft model of prostate cancer developed by injection of LNCaP cells in the flank of BALB/c nude mice. After tumors had grown to ~100 $mm^3$, we began comparative efficacy studies by dividing animals into five groups in such a manner as to minimize weight and tumor size differences among the groups. Using the MTD of 5 mg/kg for intravenous administration of our construct in Swiss albino mice as a reference point, the following regimens were administered by intravenous injections twice weekly for four weeks: (*i*) saline, (*ii*) cisplatin (1 mg/kg), (*iii*) PLGA-*b*-PEG-Apt-NP (20 mg/kg), and (*iv*) Pt-PLGA-*b*-PEG-Apt-NP (0.3 mg/kg). The tumor size and body weight were then monitored for 4 weeks. We have previously reported the preferential binding, uptake, and tumor accumulation of PSMA Apt-targeted NPs when compared to equivalent nontargeted NPs in LNCaP monolayers and LNCaP subcutaneous xenograft mouse model of PCa (6, 8); thus nontargeted NPs were not included in our efficacy study. We aimed to determine whether delivery of a Pt(IV) prodrug with Apt-targeted NPs will result in enhanced antitumor efficacy in vivo when compared to free cisplatin given in its conventional dosage form. The results showed that administration of the Pt-PLGA-*b*-PEG-Apt-NP at 0.3 mg/kg was more efficacious than control PLGA-*b*-PEG-Apt-NP at 20 mg/kg and free cisplatin at 1 mg/kg over the first 14 d. At day 12, the average tumor volume of $80.99 \pm 22.22$ $mm^3$ for the cisplatin group was significantly larger than the average tumor volume of $42.43 \pm 31.27$ $mm^3$ for the Pt-PLGA-*b*-PEG-Apt-NP group; $P < 0.05$. By day 28, the Pt-PLGA-*b*-PEG-Apt-NP at 0.3 mg/kg was equally efficacious to cisplatin at 1 mg/kg (Fig. 6*A*). The absolute weight loss difference in the cisplatin and Pt-PLGA-*b*-PEG-Apt-NP groups was modest at the doses studied in mice (Fig. 6*B*). Importantly, a previous report failed to show any improvement in the efficacy of cisplatin encapsulated PLGA-PEG NPs for prostate cancer (24). The present technology differs in two distinct ways, which in combination may explain our observed improvement in drug therapeutic index. Foremost, we delivered cisplatin in the form of a Pt(IV) prodrug, thereby enhancing its tolerability, which translated into an ability to deliver a larger amount of Pt. In addition, we employed a targeted polymeric

BIOCHEMISTRY

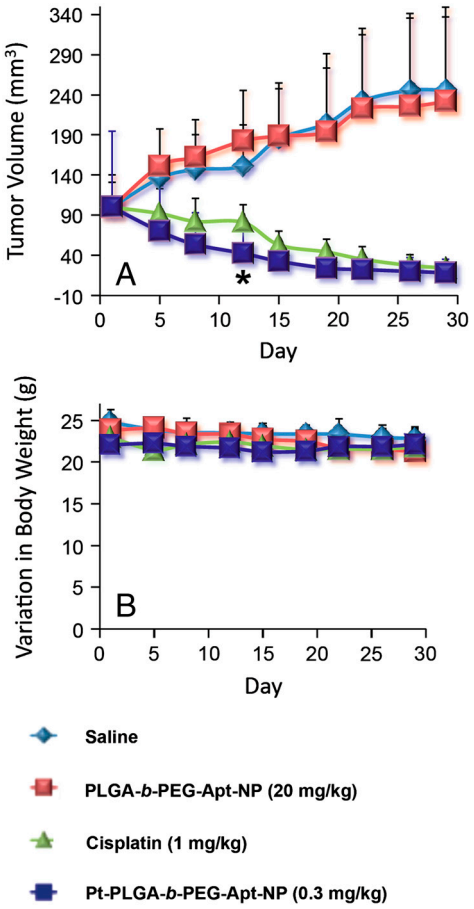


**Fig. 6.** (*A*) Effect of cisplatin (1 mg/kg), Pt-PLGA-*b*-PEG-Apt-NP (0.3 mg/kg), PLGA-*b*-PEG-Apt-NP (20 mg/kg), and saline on the growth of LNCaP tumors inoculated in nude BALB/c mice. Each formulation was administered biweekly by intravenous injection for 30 d. Mean values and standard errors of the mean are presented. Asterisk on day 12 represents significant differences between cisplatin- and Pt-PLGA-*b*-PEG-Apt-NP-treated tumors according to one-way ANOVA with Tukey post hoc test, $p < 0.05$. (*B*) Body weight changes with time of LNCaP tumor-bearing mice treated with cisplatin (1 mg/kg), Pt-PLGA-*b*-PEG-Apt-NP (0.3 mg/kg), PLGA-*b*-PEG-Apt-NP (20 mg/kg), and saline. Bars indicate standard deviations.

delivery vehicle, which we and others have shown to improve drug efficacy (6, 7, 25–29). There is significant potential in the application of targeted delivery of Pt prodrugs for cancer therapy.

## Summary

In the present investigation, the hydrophobic Pt(IV) compound **1** was used as a prodrug for delivery of cisplatin to prostate cancer using PSMA-targeted PLGA-*b*-PEG-NPs. The PLGA-*b*-PEG-Pt (IV) prodrug NPs increased the drug MTD when compared to that of cisplatin administered in its conventional dosage form in both rat and mouse models. We observed prolonged drug residence in blood when our Pt-PLGA-*b*-PEG NPs were administered to rats by i.v. injection compared to free prodrug and cisplatin administered in its conventional dosage form. Our findings using a LNCaP xenograft mouse model of PCa suggest that our system is more efficacious in reducing prostate tumors at a significantly lower dose of platinum. This study thus demonstrates an efficient, nontoxic system for the use of Pt-based chemotherapy with significant potential for treating human prostatic carcinoma in vivo and forms a basis for further development of Pt-NP-based systems for evaluation of the most effective candidates for human prostate cancer chemotherapy.

## Materials and Methods

Cisplatin was purchased from Strem Chemicals, Inc. The platinum(IV) prodrug, *c,t,c*-$[Pt(NH_3)_2(O_2CCH_2CH_2CH_2CH_2CH_3)_2Cl_2]$ (9) was synthesized as previously described. Pt(IV)-encapsulated NPs were prepared by using the nanoprecipitation method. NHS, EDC, and hexanoic anhydride were purchased from Aldrich. PLGA with acid end groups was purchased from Adsorbable Polymers International. A PEG polymer of molecular weight 3,400 with a terminal amine and carboxylic group ($NH_2$-PEG-COOH) was custom synthesized (Nektar Therapeutics). The RNA aptamer with the sequence 5′-$NH_2$-spacer GGGAGGACGAUGCGGAUCAGCCAUGUUUACGUCACUCCUUGUCAAUCCUCAUCGGCiT-3′ containing 2′-fluoro pyrimidines, a 3′-inverted T cap, and a 5′-amino group attached by a hexaethyleneglycol spacer was custom synthesized by RNA-TEC. AAS measurements were taken on a PerkinElmer AAnalyst 600 spectrometer. The NP size was obtained by quasielectric laser light scattering by using a ZetaPALS dynamic light-scattering detector (15 mW laser, incident beam = 676 nm, Brookhaven Instruments).

**Animals.** All animals were obtained from Charles River Laboratory. The animals were allowed free access to sterile food pellets and water. All in vivo studies were performed in accordance with National Institutes of Health Animal Care guidelines.

**Tumor Cells.** Androgen-sensitive human prostate adenocarcinoma LNCaP cells were obtained from American Type Culture Collection. Cells were cultured in RPMI medium 1640 (Invitrogen) with 10% fetal bovine serum, 2 mM glutamine, 50 units/mL penicillin, and 50 μg/mL streptomycin. Cells were routinely passed by treatment with trypsin (0.05%)/EDTA.

***Evaluation of maximum tolerated dose.*** Male Sprague Dawley rats and Swiss Albino mice were used to evaluate the MTD of Pt-PLGA-*b*-PEG-NPs and **1**. All groups ($n = 3$) received a single dose by intravenous injection. Four groups of rats received either cisplatin or **1** at a dose of 5, 10, 20, or 40 mg/kg. Six groups of rats received Pt(IV)-loaded NPs, Pt-PLGA-*b*-PEG-NPs with a Pt content of 5, 10, 20, 40, 50, and 60 mg/kg. The control groups received saline or 100, 200, 400, 800, and 1,000 mg/kg of empty NPs. The injection volume was 2 mL in all cases. The weight and physical states of all the rats were monitored for a period of 10 d. For the MTD studies in Swiss Albino mice, five groups ($n = 3$) of mice were given a single intravenous injection of Pt-PLGA-*b*-PEG-NP with a Pt content of 1, 3, 5, 10, or 20 mg/kg. Control mice were treated with saline and 20, 60, 100, and 200 mg/kg of PLGA-*b*-PEG-NP.

***Biodistribution and excretion study.*** The blood persistence properties of Pt-PLGA-*b*-PEG-NPs and **1** were determined using male Sprague Dawley rats weighing ~300 g. The animals, three per group, were injected in the tail vein with 2 mL of Pt-PLGA-*b*-PEG-NPs (40 mg/kg), **1** (20 mg/kg), or saline. At predetermined time intervals, blood samples were collected in preweighed heparinized tubes and centrifuged to get the plasma. The percentage of Pt was calculated by taking into consideration that blood constitutes 7% of body weight (30) and plasma constitutes 55% of blood volume. The Pt content in blood and plasma were determined by AAS.

Collective urine samples were accumulated over 24 h and stored frozen until directly analyzed by flameless AAS. Tissue samples, however, required prior digestion in concentrated nitric acid. Gentle heating was required to complete the digestion. Following evaporation to near dryness, the digests were taken up in 1 N HCl (2 mL) and again heated to near dryness to remove excess nitric acid. After repeating this last stage with 0.1 N HCl (2 mL), the digests were dissolved in 1 mL of 0.1 N HCl for Pt analysis. The method permits estimation of total Pt metal in tissue samples, and no attempt was made to identify the chemical nature of Pt species present. WinNonlin v5.2.1 NCA model 201, IV bolus software was used to calculate the pharmacokinetic parameters.

***In vivo anticancer efficacy evaluation.*** Nude BALB/c mice (6–8 wk old, male, 20 to 30 g body weight) were purchased from the Charles River Laboratory and maintained under pathogen-free conditions. The animal use protocol was approved by the Institutional Animal Care and Use (MIT and BWH) Committees on animal care. The mouse LNCaP xenograft tumor model was developed by injecting $1 \times 10^6$ cells of a 0.1 mL LNCaP cell suspension into the right flank of a BALB/c mouse using 50% matrigel. Tumor nodules were allowed to grow to a volume ~100 $mm^3$ before initiating treatment. Tumor-bearing BALB/c mice were randomly assigned to four groups. Tumor length and width were measured with calipers, and the tumor volume was calculated using the following equation:

$$\text{tumor volume}(V) = \text{length} \times \text{width} \times \text{width}/2.$$

Prior to treatment, all the mice were numbered using ear tags, and their weight and the initial tumor volume were measured and recorded. Test animals received two intravenous injections weekly at intervals of 3 or 4 d of (*i*) saline ($n = 5$), (*ii*) cisplatin (1 mg/kg) ($n = 10$), (*iii*) PLGA-*b*-PEG-Apt-NP (20 mg/kg) ($n = 5$), and (*iv*) Pt-PLGA-*b*-PEG-Apt-NP (0.3 mg/kg) ($n = 10$) formulation for four weeks, where *n* is the number of mice in each group. The injection volume was 200 μL. The weight and tumor volume of each mouse were measured twice weekly over a period of 30 d.

***Statistics*** All data were expressed as mean ± SD. Differences between groups were assessed by the one-way ANOVA. $P < 0.05$ was considered as the statistical significance level.

**ACKNOWLEDGMENTS.** This research was supported by the National Cancer Institute under Grants CA034992 (to S.J.L.) and CA119349 (to O.C.F.), by the National Institute of Biomedical Imaging and Bioengineering Grant under EB003647 (to O.C.F.), and by the Koch-Prostate Cancer Foundation Award in Nanotherapeutics (to O.C.F.). S.D. is grateful to the Koch Institute for Integrative Cancer Research for partial financial support.

1. Chen Y, Tang Y, Wang MT, Zeng S, Nie D (2007) Human pregnane X receptor and resistance to chemotherapy in prostate cancer. *Cancer Res* 67:10361–10367.
2. Jamieson ER, Lippard SJ (1999) Structure, recognition, and processing of cisplatin-DNA adducts. *Chem Rev* 99:2467–2498.
3. Rosenberg B, VanCamp L, Trosko JE, Mansour VH (1969) Platinum compounds: A new class of potent antitumour agents. *Nature* 222:385–386.
4. Galanski M, Jakupec MA, Keppler BK (2005) Update of the preclinical situation of anticancer platinum complexes: Novel design strategies and innovative analytical approaches. *Curr Med Chem* 12:2075–2094.
5. Wang D, Lippard SJ (2005) Cellular processing of platinum anticancer drugs. *Nat Rev Drug Discov* 4:307–320.
6. Farokhzad OC, et al. (2006) Targeted nanoparticle-aptamer bioconjugates for cancer chemotherapy in vivo. *Proc Natl Acad Sci USA* 103:6315–6320.
7. Farokhzad OC, et al. (2004) Nanoparticle-aptamer bioconjugates: A new approach for targeting prostate cancer cells. *Cancer Res* 64:7668–7672.
8. Gu F, et al. (2008) Precise engineering of targeted nanoparticles by using self-assembled biointegrated block copolymers. *Proc Natl Acad Sci USA* 105:2586–2591.
9. Dhar S, Gu FX, Langer R, Farokhzad OC, Lippard SJ (2008) Targeted delivery of cisplatin to prostate cancer cells by aptamer functionalized Pt(IV) prodrug-PLGA-PEG nanoparticles. *Proc Natl Acad Sci USA* 105:17356–17361.
10. Israeli RS, Powell CT, Fair WR, Heston WW (1993) Molecular cloning of a complementary DNA encoding a prostate-specific membrane antigen. *Cancer Res* 53:227–230.
11. Murphy GP, Elgamal AA, Su SL, Bostwick DG, Holmes EH (1998) Current evaluation of the tissue localization and diagnostic utility of prostate specific membrane antigen. *Cancer* 83:2259–2269.
12. Kawakami M, Nakayama J (1997) Enhanced expression of prostate-specific membrane antigen gene in prostate cancer as revealed by in situ hybridization. *Cancer Res* 57:2321–2324.
13. Wright GL, Jr, et al. (1996) Upregulation of prostate-specific membrane antigen after androgen-deprivation therapy. *Urology* 48:326–334.
14. Chang SS, et al. (1999) Five different anti-prostate-specific membrane antigen (PSMA) antibodies confirm PSMA expression in tumor-associated neovasculature. *Cancer Res* 59:3192–3198.
15. Alexis F, Pridgen E, Molnar LK, Farokhzad OC (2008) Factors affecting the clearance and biodistribution of polymeric nanoparticles. *Mol Pharmaceut* 5:505–515.
16. Gref R, et al. (1994) Biodegradable long-circulating polymer nanospheres. *Science* 263:1600–1603.
17. Dhar S, Liu Z, Thomale J, Dai H, Lippard SJ (2008) Targeted single-wall carbon nanotube-mediated Pt(IV) prodrug delivery using folate as a homing device. *J Am Chem Soc* 130:11467–11476.
18. Mukhopadhyay S, et al. (2008) Conjugated platinum(IV)-peptide complexes for targeting angiogenic tumor vasculature. *Bioconjugate Chem* 19:39–49.
19. Dhar S, Lippard SJ (2009) Mitaplatin, a potent fusion of cisplatin and the orphan drug dichloroacetate. *Proc Natl Acad Sci USA* 106:22199–22204.
20. Kolishetti N, et al. (2010) Engineering of self-assembled nanoparticle platform for precisely controlled combination drug therapy. *Proc Natl Acad Sci USA* 107:17939–17944.
21. Siddik ZH, Jones M, Boxall FE, Harrap KR (1988) Comparative distribution and excretion of carboplatin and cisplatin in mice. *Cancer Chemother Pharmacol* 21:19–24.
22. Wang S, et al. (2003) Pharmacokinetics and tissue distribution of iv injection of polyphase liposome-encapsulated cisplatin (KM-1) in rats. *Acta Pharmacol Sin* 24(6): 589–592.
23. Avgoustakis K, et al. (2002) PLGA-mPEG nanoparticles of cisplatin: In vitro nanoparticle degradation, in vitro drug release and in vivo drug residence in blood properties. *J Control Release* 79:123–135.
24. Mattheolabakis G, Taoufik E, Haralambous S, Roberts ML, Avgoustakis K (2009) In vivo investigation of tolerance and antitumor activity of cisplatin-loaded PLGA-mPEG nanoparticles. *Eur J Pharm Biopharm* 71:190–195.
25. Gu F, Langer R, Farokhzad OC (2009) Formulation/preparation of functionalized nanoparticles for in vivo targeted drug delivery. *Methods Mol Biol* 544:589–598.
26. Bagalkot V, Farokhzad OC, Langer R, Jon S (2006) An aptamer-doxorubicin physical conjugate as a novel targeted drug-delivery platform. *Angew Chem Int Edit* 45:8149–8152.
27. Sajja HK, et al. (2009) Development of multifunctional nanoparticles for targeted drug delivery and noninvasive imaging of therapeutic effect. *Curr Drug Discov Technol* 6:43–51.
28. Huang YF, et al. (2009) Molecular assembly of an aptamer-drug conjugate for targeted drug delivery to tumor cells. *ChemBioChem* 10:862–868.
29. Zhao X, Li H, Lee RJ (2008) Targeted drug delivery via folate receptors. *Expert Opin Drug Del* 5:309–319.
30. Lee HB, Blaufox MD (1985) Blood volume in the rat. *J Nucl Med* 26:72–76.